EPA Public Access
Author manuscript
Tree Physiol. Author manuscript; available in PMC 2019 May 20.
About author manuscripts | Submit a manuscript

Published in final edited form as:
Tree Physiol. 2018 April 01; 38(4): 630–640. doi:10.1093/treephys/tpx120.

Polyploidy influences plant-environment interactions in Quaking Aspen (*Populus tremuloides* Michx.)

Burke T. Greer[1,2,*], **Christopher Still**[1,2], **Grace L. Cullinan**[2,3], **J. Renée Brooks**[4], and **Frederick C. Meinzer**[5]

[1]Forest Ecosystems and Society, College of Forestry, Oregon State University, 321 Richardson Hall, Corvallis, Oregon 97331, USA. 415-680-6430

[2]Rocky Mountain Biological Laboratory, P.O. Box 519, Crested Butte, CO, Colorado 81224, USA

[3]Rice University, Biosciences at Rice, Ecology and Evolutionary Biology Department, 6100 Main St. Houston, TX 77005

[4]U.S. Environmental Protection Agency, National Health and Environmental Effects Research Laboratory, Western Ecology Division, 200 SW 35th St, Corvallis OR 97333, USA

[5]USDA Forest Service Pacific Northwest Research Station, 3200 SW Jefferson Way, Corvallis, OR 97331, USA

Abstract

Quaking aspen (*Populus tremuloides* Michx.), a widespread and keystone tree species in North America, experienced heat and drought stress in the years 2002 and 2003 in the Southwestern United States. This led to widespread aspen mortality that has altered the composition of forests, and is expected to occur again if climate change continues. Understanding interactions between aspen and its environments is essential to understanding future mortality risk in forests. Polyploidy, which is common in aspen, can modify plant structure and function and therefore plant-environment interactions, but the influence of polyploidy on aspen physiology is still not well understood. Furthermore, the ploidy types of aspen have different biogeographies, with triploids being most frequent at lower latitudes in generally warmer and drier climates, while the northerly populations are virtually 100% diploid. This suggests that ploidy-environment interactions differ, and could mean that the ploidy types have different vulnerabilities to environmental stress. In this study, to understand aspen ploidy-environment interactions, we measured 38 different traits important to carbon uptake, water loss, and water-use efficiency in diploid and triploid aspen in Colorado. We found that triploid aspen had lower stand density, and greater leaf area, leaf mass, leaf mass per area, % nitrogen content, chlorophyll content, and stomatal size. These differences corresponded to greater potential net carbon assimilation (A, measured using A/C_i curves, and chlorophyll fluorescence) and stomatal conductance (g_s) in triploids than diploids. While triploid aspen had higher intrinsic water-use efficiency (iWUE, calculated from measurements of $\delta^{13}C$ in leaf tissue), they also had greater potential water loss

*Corresponding Author.

Conflict of Interest:
None declared

EPA Author Manuscript
EPA Author Manuscript
EPA Author Manuscript

from higher measured g_s and lower stomatal sensitivity to increasing vapor pressure deficit. Therefore, despite greater iWUE, triploids may have lower resilience to climate-induced stress. We conclude that ploidy type strongly influences physiological traits and function, and mediates drought stress responses in quaking aspen.

Keywords

ecophysiology; evolutionary ecology; climate stress; intrinsic water-use efficiency; photosynthesis; stomatal conductance

Introduction

Quaking aspen (*Populus tremuloides* Michx.), a native and keystone tree species in North America, grows in a wide variety of landscapes and environments including interior Alaska, Newfoundland, the Great Lakes Region, the Western United States, Mexico, and many places in between. This widespread biogeography is driven, in part, by aspen having high phenotypic plasticity, wind dispersed seeds, and the ability to clone asexually through root suckering (Mitton and Grant 1996). Root suckering allows for rapid and widespread growth once established, and in some cases individual aspen clones can be enormous (Kemperman and Barnes 1976, Mitton and Grant 1996, Mock et al. 2008). For example, the world's largest organism by biomass is thought to be an aspen clone that contains over 47,000 individual ramets and extends over 43 ha in area (Kemperman and Barnes 1976, Mock et al. 2008). However, despite a broad species niche, and clonal growth, quaking aspen can be very susceptible to environmental stressors.

Lower than normal precipitation and above average temperatures across Colorado, Utah, Arizona, and New Mexico in the years 2002 and 2003 led to substantial and widespread aspen mortality, known as Sudden Aspen Decline (SAD). SAD-affected aspen had embolized xylem conduits that either led directly to mortality or instead weakened trees because of diminished whole-ramet hydraulic conductance and reduced intrinsic water-use efficiency (Anderegg et al. 2013a, Anderegg et al. 2014, Anderegg et al. 2012, Anderegg et al. 2013b). Because of SAD, there has been a massive shift in the composition of some forests in the southwestern United States. In the front range of Colorado, for example, a recent survey of plots first sampled in 1972–1973 (Peet 1981) showed that 22 of 89 plots that previously had aspen no longer contain aspen, and where aspen remain, there are fewer aspen in all size classes (Bretfeld et al. 2016). Also, in a separate study near Crested Butte, Colorado on the western slope of the Rocky Mountains, aspen stand density and basal area decreased by 32% between 1964 and 2010, likely in response to both SAD and browsing by ungulates (Coop et al. 2014). Furthermore, the largest aspen clone, known as Pando, has recently had low recruitment of new ramets driven by climate stress and herbivory (Rogers and Gale 2017). This is noteworthy, as the Pando clone, and others like it, are thought to be thousands of years old and reliant on asexual reproduction (Ally et al. 2010, Mitton and Grant 1996). Climate change scenarios predict that both temperatures and drought stress will increase in the Western United States (Worrall et al. 2013), and we should expect that aspen will experience SAD-like mortality events again in the future.

EPA Author Manuscript EPA Author Manuscript EPA Author Manuscript

EPA Author Manuscript EPA Author Manuscript EPA Author Manuscript

Understanding interactions between quaking aspen and climate is essential to forecasting SAD events, but one critical dynamic to aspen-climate interactions is not well understood: polyploidy. Polyploidy is important in plants because the duplicated genomes of polyploids can alter gene expression and therefore the expression of phenotypic structural and functional traits that drive plant-environment interactions (Barker et al. 2016, Madlung and Wendel 2013, Maherali et al. 2009, Segraves and Anneberg 2016, Soltis et al. 2014). For example, polyploids of *Betula papyrifera* have been found to have leaves containing smaller stomata, more stomata per unit leaf area, a thicker epidermis, and increased leaf pubescence – all traits that tend to reduce water loss (Li et al. 1996). Additionally, during a 2-hour water stress treatment, diploid *Betula papyrifera* reduced net photosynthesis and stomatal conductance more and maintained less negative water potentials than polyploids (Li et al. 1996). These differences between ploidy types in *Betula papyrifera* also likely drive the different ploidy-type biogeographies in this species: diploids are more often found in cooler and wetter environments than polyploids (Li et al. 1996). In quaking aspen, diploids and triploids also have also been found to have different distributions: triploids were most frequently found at lower latitudes in warmer and drier climates with the remaining cooler and wetter portion of the species' range being virtually 100% diploid (Mock et al. 2012). Triploid quaking aspen have also been found to have greater basal area increments over time than diploids, which could be explained by differences in structure and function between the ploidy types (DeRose et al. 2014, Mock et al. 2012, Mock et al. 2008). European aspen (*Populus tremula* L.) triploids have been found to grow faster than their diploid counterparts because triploids have higher quantum yields of CO_2 fixation, and greater rates of light-saturated net photosynthesis than diploids (Pärnik et al. 2014). However, beyond differences in distribution and BAI relative to climate, intrinsic physiological differences between aspen ploidy types, or differences in aspen ploidy-environment interactions or climate tolerances, have not been well quantified or understood. We speculate that these factors are important to aspen forest resilience to climate change and past and/or future mortality events caused by heat and drought stress (Worrall et al. 2013). In this study, to assess how polyploidy might influence aspen-environment interactions of co-occurring diploid and triploid aspen in a natural aspen forest in Colorado, we measured and compared ploidy differences in aspen clone, ramet, and leaf traits, as well as photosynthesis, stomatal conductance, and leaf carbon isotope composition and intrinsic water use efficiency.

Methods

Study Site

The study site (38.716 N, 106.819 W) was a 2.5 km^2 naturally occurring aspen forest near Almont, Colorado, and the Rocky Mountain Biological Laboratory (in Gothic, Colorado) at 2750 meters in elevation (Figure 1). The climate measured at three nearby weather stations (Crested Butte, Gunnison, and Taylor Park) shows that the 1980–2014 average May to September temperature was 11.3°C, and the October to April mean temperature was −5.2°C. The 1980–2014 May to September average total precipitation was 19.1 cm, while the October to April average total precipitation was 21.6 cm (Global Historical Climate Network Dataset (GHCN), http://www.ncdc.noaa.gov/cdo-web/).

EPA Author Manuscript

EPA Author Manuscript

EPA Author Manuscript

Study and Statistical Design

We compared physiological and morphological traits in five pairs of diploid and triploid clones found throughout the stand (Figure 1). An individual quaking aspen clone consists of multiple stems (ramets) that have grown from root suckering (Mitton and Grant 1996). Individual clones were visually identified throughout the stand and tested for ploidy level using flow cytometry (see below for details). Five diploid and five triploid clones were then selected for continued study. Each clone was spatially segregated from other clones of similar ploidy to ensure they were independent clones. Because a single aspen clone actually consists of multiple ramets, we chose to represent a clone using measurements in five separate ramets in each clone. For each clone, we selected ramets whose bark and leaf color and size were similar and were growing within 20 meters of each other to ensure that each ramet was a member of the same clone. Clones were selected in pairs (with similar proximity) to minimize any potential within-site differences driven by geology, soil type, and soil depth. This paired design allowed us to alternate between clone pairs of differing ploidy for instantaneous physiological measurements that might fluctuate with ambient conditions (see below for details).

Linear mixed models created using R version 3.3.1 (R Core Team 2013) and the nlme R package (Pinheiro et al. 2017) were used for statistical comparisons between the ploidy types. The variable of interest was the dependent variable, and ploidy type was the fixed effect in each model. For our analysis, we used a hierarchical statistical framework wherein leaf measurements were nested within a ramet, and ramet measurements were nested within a clone. The random effect was set depending on the scale of the measurement. Leaf-scale measurements were taken within each clone's ramets; therefore, in the mixed models, the clone means for leaf-scale measurements were estimated using a random effect of ramet nested within clone. For ramet-scale measurements, clone identity was the random effect. Restricted maximum likelihood (REML) was used to fit the models, and we ensured that model assumptions were met, and that residuals were evenly distributed. If residuals showed any patterns (including uneven spread over the fitted values), we adjusted the model to allow residuals to differ between groups, or by choosing alternative correlation structures to improve the model fit (see Appendix S1). To evaluate if the means of our measurements differed by ploidy type, we compared the means using F-tests of overall significance, using a threshold of $\alpha = 0.05$.

Ploidy Identification

The ploidy type of multiple clones was tested using flow cytometry before choosing clones for continued study. We used similar methods to the protocol used by Mock et al. (2012) to identify diploid (2n = 2x = 38) and triploid (2n = 3x = 57) clones. Briefly, fresh leaf samples were dried using silica gel (Activa Flower Drying Art Silica Gel) and from each dried sample, 1 cm^2 sized sections were chopped with equally sized fresh samples of diploid *Hordeum vulgare* (1C genome size is 5.55 pg (Bennett and Leitch 2012)). Nuclei were suspended and stained using the CyStain® PI Absolute T kit produced by Partec. For nuclei extraction, 150 μl of extraction buffer (with 2% by volume polyvinylpyrrolidone) was added to the chopped leaf material. Then, the suspension was filtered using disposable tube top filters (CellTrics, Sysmex Partec, Görlitz, Germany) and 750 μl of stain (CyStain, Sysmex

EPA Author Manuscript

EPA Author Manuscript

EPA Author Manuscript

Partec, Görlitz, Germany) was added. Filtrates were analyzed using a flow cytometer (Accuri C6, BD Biosciences, Franklin Lakes, NJ, USA) and excited using a 585 nm wavelength laser. Boxplots of the ratios of the median peak fluorescence of each aspen sample relative to the *H. vulgare* peak fluorescence were used to determine the ploidy of each ramet (Figure 2). Triploid aspen, having an extra set of chromosomes, should have 50% more fluorescence than diploids, and we assigned ploidy accordingly. In addition, we also tested the ploidy of several samples provided by K. Mock (Utah State University) with known ploidy and found 100% correspondence between ploidy determinations.

Clone, Ramet and Leaf Characteristics

Characteristics at the level of clone, ramet, and leaf were measured. First, aspen clone structure, an indicator of the potential degree of water and light resource competition between ramets, was measured in July of 2014 and July of 2015. Clone basal area per ground area and canopy openness (percent open sky) were measured once per clone using a wedge prism, and a spherical densiometer, respectively.

Ramet diameter at 1.3 meters above ground elevation (DBH) in five ramets of each clone was measured. The height of each ramet was also measured using a laser range finder. Leaf area index (LAI) of four ramets in each clone was measured using an LAI meter (LAI-2000, LI-COR Biosciences, Lincoln, NE, USA) between first light and dawn. Because clone canopy openness was heterogeneous, LAI measurements were taken for each ramet by averaging LAI measured across four equally spaced measurements (separated by 90 degrees around the ramet) 1.3 meters above ground, and 3 meters away from the stem using the 50% lens cover with the open portion facing the aspen stem. Thus, while LAI is typically considered a stand level measurement, these measurements were made for specific ramets over a standardized total ground area around each tree.

Within each ramet, leaf size (area per leaf) was measured on at least ten fresh and healthy, sunlit, leaves from the lower crown by using ImageJ on digital scans of these leaves (Schneider et al. 2012). Oven-dried mass of healthy leaves was also measured in the leaves used for leaf area. Leaf size and mass were averaged by ramet. Leaf mass per area (LMA) was calculated as dry leaf mass normalized by leaf size. In addition, stomatal sizes (measured as the length of the stomatal guard cells) and densities were measured using a digital microscope (VHX-1000E, Keyence Corporation, Osaka, Japan) in leaf peels collected in the field by coating the abaxial surface with fast-drying nail polish, and allowing the nail polish to set for ten minutes. We then removed the nail polish using clear tape, and immediately affixed the leaf peels to clear slides.

Photosynthetic Rates and Chlorophyll Fluorescence

Photosynthetic properties of leaves in diploid and triploid ramets were also measured. Because photosynthetic rates are modulated by environmental conditions, measurements were alternated between diploid and triploid ramets from paired diploid and triploid clones over a single day (between 09:00 and 14:00), and captured over 5 separate days to characterize all five clone pairs. In July of 2015, the relative chlorophyll content of aspen leaves was estimated using a SPAD meter (SPAD 502 Plus, Spectrum Technologies, Aurora,

EPA Author Manuscript EPA Author Manuscript EPA Author Manuscript

IL, USA) as the average SPAD of 20 leaves for each ramet. A SPAD meter measures leaf transmittance of red (650 nm) and infrared (940) light and produces a unitless SPAD measurement as an estimate of "greenness" (Ling et al. 2011). We measured A/C_i curves (net CO_2 assimilation rate, A, versus calculated substomatal CO_2 concentration, C_i) and chlorophyll fluorescence to examine photosynthetic physiology in diploid and triploid aspen. For A/C_i measurements, we used an integrated chlorophyll fluorimeter and gas exchange unit (i*FL,* Opti-sciences Inc, and ADC BioScientific Limited) with a broadleaf chamber. During June of 2016, we measured three leaves on three different ramets per clone, again alternating between clone pairs during the measurements. The dependence of A on Ci was measured by sequentially controlling the CO_2 concentration of air in the leaf chamber between 50 and 1600 ppm. Before taking measurements, the leaf was placed in the chamber, which was set to match ambient conditions, and the chamber was allowed to stabilize. Afterwards, chamber conditions were set so that photosynthetic photon flux density (PPFD) was saturating at 1,500 μmol m^2s^{-1}, the chamber temperature was 25°C, the vapor pressure was 1.47 kPa, and the mass flow of air per m^2 of leaf area was 200 (mol m^{-2} s^{-1}). Then CO_2 concentrations were sequentially adjusted to 400, 300, 200, 100, 50, 200, 400, 600, 800, 1000, 1200, and 1600 ppm. These adjustments were made after measurements of each chamber CO_2 concentration and ΔCO_2 stabilized between steps. At each step, A (μmol m^2s^{-1}) was measured, and C_i was calculated (see Appendix S2 for more details on C_i calculations).

The resulting A/C_i curves were fit to the data using the 'plantecophys' R package and the data points collected where CO_2 concentrations increased from 50 ppm to 1600 ppm. Curves were fit using the 'default' method, without temperature correction (the chamber temperature was maintained at 25°C for each curve). Curve fitting followed the A/C_i model (Farquhar et al. 1980, Harley et al. 1992, Harley and Sharkey 1991, Sharkey 1985) where the carboxylation rate during photosynthesis is limited by: 1) the maximum rate of Rubisco-catalyzed carboxylation (termed "Rubisco-limited", V_{cmax}); 2) the regeneration of ribulose biophosphate (RuBP, or J_{max}), which is regulated by the electron transport rate, J; and 3) the regeneration of RuBP as controlled by the rate of triose-phosphate utilization (TPU). Dark respiration in the light (R_d), the CO_2 compensation point (Γ^*), and K_m (half of the rate at which CO_2 update is maximized) were derived from these curves and compared between ploidy types.

Leaf fluorescence, an indicator of photosystem II (PSII) capacity and efficiency, was measured as using a MINI-PAM (Walz, Effeltrich, Germany). These measurements provided the quantum yield of photosystem II (Φ_{PSII}) and the electron transport rate (J) of diploid and triploid aspen (see Appendix S2 for more details) calculated from background fluorescence (F_t) and maximum fluorescence (F'_m). The maximum quantum yield of PSII (Φ_{PSII}) in the light was calculated as:

$$\Phi_{PSII} = \left(F'_m - F_t\right)/F'_m$$

EPA Author Manuscript

EPA Author Manuscript

EPA Author Manuscript

In dark-adapted leaves Φ_{PSII} can estimate the maximum potential quantum efficiency because in dark conditions photosystem II reaction centers should all be 'open'. Φ_{PSII}in dark-adapted leaves is also an indicator of plant photosynthetic performance and can indicate plant stress (Maxwell and Johnson 2000). Φ_{PSII}can also be utilized to estimate the electron transport rate (J) and therefore overall photosynthetic capacity in vivo:

$$J = \Phi_{PSII} * PFDa * 0.5$$

where PFDa is absorbed light and 0.5 is a factor representing the partitioning of energy between photosystem I and photosystem II. Rapid light curves (RLCs) are successive measurements of Φ_{PSII} under increasing quantities of actinic light, and the initial slopes and maximum yields of both Φ_{PSII} and J from RLCs provided useful information about the efficiency of photosystem II, electron transport, and the maximum light that a leaf can use to drive photosynthesis.

Both the maximum quantum yield of PSII in the dark and RLCs in the light were measured. During July of 2015, between the hours of 03:00 and 05:00, twenty measurements per ramet of F_0 and F_m were collected in the dark. In July of 2015 and June of 2016, under ambient light conditions between 10:00 and 14:00, RLCs were measured in three sunlit leaves in each of the 50 ramets. RLCs were alternated between paired diploid and triploid clones over 5 days, and conducted on sunlit leaves that were shaded by a clipboard during the RLC to achieve lower-than-ambient lighting conditions required for the RLC (the sunny day maximum was generally between 1800 and 2200 μmol m^{-2} s^{-1}). The minimum and maximum fluorescence (F_t and F'_m) were measured at eight different light levels following a saturating pulse.

Curves were fit to each RLC measurement of Φ_{PSII} (measured in daytime RLCs) using non-ordinary least squares based on equation 2 from Thornley (2002) that estimates the quantum yield of photosynthesis and the maximum light-saturated photosynthetic rate:

$$\Phi_{PSII}\left(I_L\right) = \frac{1}{2\xi}\left(\alpha I_L + ETR_{max} - \sqrt{[(\alpha I_L + ETR_{max})^2 - 4\xi\alpha I_L ETR_{max}]}\right)$$

We estimated two parameters of this equation: α, the electron transport efficiency (or the initial slope of the $\Phi_{PSII}\left(I_L\right)$ curve), and ETR_{max} (the light-saturated photosynthetic rate). I_L was the incident PAR (μmol PAR $m^{-2}s^{-1}$) during the RLC. ξ is the sharpness of the 'knee' of the curve and was set to 0.9. We estimated α and ETR_{max} using the nls2 package in R using the least squares method. During our statistical tests, we tested for significant differences for the $\log(\Phi_{PSII})$ between the ploidy types for the combined data, and for differences in α and ETR_{max} derived from individual RLCs.

EPA Author Manuscript

EPA Author Manuscript

EPA Author Manuscript

Stomatal Conductance

Stomatal conductance (g_s) was measured in both clones in July of 2014, and again in June and July of 2015 using a leaf porometer (SC-1, Decagon Devices Inc., Pullman, WA, USA) in three sunlit leaves per ramet on the abaxial surface of each leaf. Because vapor pressure deficit (D) can drive changes in g_s (Collatz et al. 1991, Hogg and Hurdle 1997, Jarvis 1976), we also calculated D from measured temperature and relative humidity at a nearby weather station (38° 39’ 17” N, 106° 51’ 42” W, 2500 meters in elevation, 7 km to the southwest) operated by the Rocky Mountain Biological Laboratory. D for each g_s measurement was matched from the closest climate measurement to observations in time. Climate station measurements were recorded every hour in 2014 and every 10 minutes in 2015.

Leaf-Specific Hydraulic Conductivity

The hydraulic conductivity (K_h) of small branches of diploid and triploid ramets was measured in June of 2016. Like many of the previous measurements, K_h measurements were paired between diploid and a triploid clones over 5 days. We took one terminal portion of a lateral branch segment from four different ramets in each diploid and triploid clone (with 40 total measurements across all clones). The branch segments (5 mm diameter and 5 cm length) were clipped from the lower sunlit canopy, and immediately placed in a water-filled tube. Just prior to the measurement, the branch was removed from the water tube while underwater in a deep dish, submerged for 15 minutes, and then recut. Afterwards, the bark was peeled from around both ends of the segment. We then measured K_h using a high pressure flow meter (Tyree et al. 1995), recording our final measurements when the difference between upstream and downstream pressures was stable for 15 minutes (the mean downstream pressure was 0.22 MPa and the mean difference in pressure was 0.04 MPa). All measurements were corrected to 20°C to account for temperature effects on the viscosity of water. Afterwards, we normalized K_h by xylem cross-sectional area (K_s) and by leaf area distal to the branch segment (K_l).

Intrinsic Water-use Efficiency

Intrinsic water-use efficiency (iWUE), the ratio of A to g_s, was calculated from measurements of carbon isotope ratios, $\delta^{13}C$, in leaf tissue. iWUE was defined as (Seibt et al. 2008):

$$iWUE = \frac{A}{g_s} = \frac{\left(C_a - C_i\right)}{1.6},$$

where C_a is the atmospheric [CO_2], and C_i is the intercellular [CO_2]. C_i was derived from measurements of $\delta^{13}C$ following the model of Farquhar et al. (1982):

$$\delta^{13}C = \delta^{13}C_a - a - (b-a)\left(\frac{C_i}{C_a}\right),$$

EPA Author Manuscript EPA Author Manuscript EPA Author Manuscript

where, $\delta^{13}C_a$ is the carbon isotope ratio in the atmosphere, a is the fractionation against $^{13}CO_2$ during molecular diffusion through the stomata (~4.4‰), and b is net fractionation due to carboxylation by the Rubisco enzyme (−27‰). For C_a and $\delta^{13}C_a$, we used the mean June and July 2014 $\delta^{13}C_a$ and C_a of air measured at Niwot Ridge, Colorado (White and Vaughn 2011). $\delta^{13}C$ was measured in pooled samples of ground leaf material from each ramet, using continuous-flow isotope ratio mass spectrometry (DeltaPlus, Thermo Fisher Scientific, Waltham, MA, USA) connected to an elemental analyzer (NA1500, CARLO ERBA, Cornaredo MI, Italy) at Oregon State University's Stable Isotope lab in Corvallis, Oregon. We also measured %N and %C in these leaf samples. Standard errors of 11 replicates for the measurements of $\delta^{13}C$, %N, and %C were +/− 0.2 ‰, 0.1%, and 0.1%, respectively.

Results

Stand and Leaf Traits

Basal area per unit ground area was significantly greater in diploid (17.5 m^2 ha^{-1}) than in triploid clones (11.4 m^2 ha^{-1}) at the clone scale (Table 1). However, the mean DBH (10.9 cm) and height (5.0 m) of the ramets did not differ between ploidy levels. Using the mean DBH, and the mean basal area per unit ground area, we also calculated that, on average, diploid clones had 1914 trees per ha, and triploid aspen had 1188 trees per ha. Nevertheless, canopy openness was similar between ploidy types (mean = 28% open).

Several leaf traits differed between the ploidy types (Table 2). Triploid leaves were nearly twice the size of diploid leaves with 76% greater overall dry mass and slightly (12%) greater LMA. LAI and the leaf areas distal to the segments used for measurements of K_l and K_s were similar across ploidy levels and because diploids had smaller leaves, triploids likely also had fewer leaves. Stomata were also 35% longer in triploids than in diploids. Leaf stomatal density was not different between ploidy types ($p < 0.50$). We used the mean stomatal length measurements to predict diploid and triploid stomatal area and average stomatal area per leaf: assuming that each stomata was an ellipse and that its width was half of the length, the mean area per stomate for triploids was nearly twice that of diploids (1742 μm^2 and 958 μm^2, respectively). By combining leaf size of diploids and triploids (13.4 cm^2 and 21.1 cm^2, respectively), with their stomatal areas, the average total stomatal area per leaf for triploids was approximately three times that for a diploid leaf (diploids = 0.7 cm^2 and triploids = 1.9 cm^2). Remembering that LAI was not significantly different between ploidy levels, the total stomatal pore area per ramet for triploids was greater for the same leaf area. These findings illustrate a tradeoff between leaf size and number on each ramet – diploid and triploids converged on a similar total leaf area per ramet, but triploids had a greater total stomatal area.

Physiology

We observed that g_s in triploids was less sensitive to changes in vapor pressure deficit (D) ($p < 0.01$, Figure 3, per Oren et al. (1999)). At high D, triploid aspen had higher stomatal conductance than diploid aspen, but at low D, diploid and triploid aspen had similar stomatal

EPA Author Manuscript EPA Author Manuscript EPA Author Manuscript

conductance values. Diploids were also more sensitive to increasing D, as indicated by a greater slope ($\frac{d(g_s)}{d(logD)}$) than triploids. Interestingly, K_s and K_l were similar between the ploidy types, though triploids trended higher in each measurement. It is possible that with greater sample numbers, K_s and K_l would be significantly different between diploids and triploids (see Appendix S3).

We observed that SPAD was 28% greater in triploids than in diploids (Table 2), reflecting greater chlorophyll content in triploids. We anticipated that photosynthetic rates and chlorophyll fluorescence would also show ploidy type differences (see Table 3). Indeed, J_{max} trended higher in triploids ($p = 0.10$, Table 3), but did not reach our threshold for statistical significance of $\alpha = 0.05$. V_{cmax}, R_d, Γ^*, and K_m derived from the A/C_i curves were not different between ploidy types (Table 3).

Φ_{PSII} in dark-adapted leaves was similar between ploidy levels ($p < 0.32$) with a mean across all diploid and triploid clones of 0.88, which is 5% higher than the more typical 0.84 found for dark-adapted Φ_{PSII}. In addition, we found that $\log(\Phi_{PSII})$ in the light depended on both ploidy type and PAR ($p < 0.01$, Figure 4). From our mixed model, we found that the slope ($\frac{d(\log(\Phi_{PSII}))}{d(PAR)}$) of diploids was greater (more negative) than triploids, suggesting that the quantum efficiency of diploids was lower than triploids. In addition, triploids had a higher maximum quantum efficiency at high light, suggesting they had more 'open' reaction centers than diploids under these conditions, possibly because they had higher chlorophyll content in their leaves. We also fit a linear mixed model to J, but did not find significant differences between ploidy types.

α and ETR_{max} from RLCs were not significantly different between the ploidy types for 2015, but triploids were 41% greater in 2016 ($p < 0.06$) in a subset of 3 diploid-triploid pairs sampled opportunistically while taking A/C_i curves.

iWUE

$\delta^{13}C$, and calculated C_i, C_i/C_a, and iWUE were all different between diploid and triploid aspen (Table 4), with triploid aspen having 12% greater iWUE. Percent nitrogen content was also 8% greater in triploids than in diploids ($p < 0.06$) which suggested that these triploids had higher photosynthetic rates. A higher nitrogen content in triploids also corresponded to greater chlorophyll content (SPAD), J_{max}, and $\log(\Phi_{PSII})$ in triploids. Leaf C:N ratio in triploids was 9% lower than diploids. Metrics of leaf N content (Table 4) revealed that the average mass of leaf nitrogen per leaf area was 20% greater in triploids than diploids and total average mass of nitrogen per leaf was 91% greater in triploids. The average mass of leaf nitrogen per ground area was 5% greater in triploids, but not significantly different ($p < 0.84$).

EPA Author Manuscript

EPA Author Manuscript

EPA Author Manuscript

Discussion

Diploid and triploid aspen clones differed significantly in physiology, structure and function that may influence ploidy-environment interactions. Many trait differences were obvious in the field: diploids had a higher ramet density per ground area, while triploid leaves were greener and larger (Figure 5). Our measurements confirmed these field observations: diploids had smaller leaves with less chlorophyll, lower LMA, and a corresponding lower leaf %N, N content (mmols m^{-2}), J_{max}, Φ_{PSII}, and g_s. We also found that iWUE was also lower in diploid leaves. These findings suggest that structural differences between the ploidy types lead to differences in plant function in response to the environment.

Structural differences between the ploidy types could explain, in part, the measured differences in g_s and iWUE. Leaves with smaller stomata and greater stomatal density typically have higher maximum g_s. In addition, leaves with higher g_s at low D usually have a greater sensitivity to increasing D (Drake et al. 2013, Franks et al. 2009, Lawson and Blatt 2014, Oren et al. 1999). While stomatal density was similar between ploidy types, diploid aspen had smaller stomata, but lower overall g_s, lower g_s at high D, and greater sensitivity to increasing D (i.e., a more negative slope). Conversely, triploid leaves with larger stomata maintained higher g_s at high D and had lower sensitivity to increasing D than diploids. Because boundary layer conductance is mediated by leaf size, as well as wind speed, we considered that triploids, despite high g_s, might have transpiration rates that are similar to diploids because of greater leaf size and lower boundary layer conductance. However, modeling the boundary layer conductance in aspen leaves is complicated by leaf flutter. The trembling motion of aspen leaves could either increase boundary layer conductance because of increased mixing with the atmosphere, or trembling leaves could instead lower leaf temperature that could instead reduce boundary layer conductance. In fact, the flutter rate of aspen leaves, which is driven by factors like leaf size, and canopy structure, could possibly be a greater control on boundary layer conductance than leaf size alone (Roden 2003, Roden and Pearcy 1993a, Roden and Pearcy 1993b, Roden and Pearcy 1993c). We also considered that triploids could have had reduced total transpiration per ramet by having lower total leaf area per ramet (total ramet transpiration = transpiration per leaf area times total ramet leaf area), but LAI was similar between ploidy types in the trees we measured. If we assume that boundary layer conductance is the same between the ploidy types because of leaf flutter, we conclude that transpiration rates are also cumulatively higher in triploid ramets. Potentially, this also explains lower stem densities in triploid clones: by having fewer ramets per ground area, triploid ramets could have greater root-to-shoot ratios than diploid ramets (which would spread limited ground water resources to fewer ramets). But the extent to which water is shared within a clone is unknown.

Despite triploids having higher g_s rates (and inferring that they have higher ramet-scale transpiration), we found that iWUE was also greater in triploids, which, in conjunction with measurements of leaf N, J_{max} and Φ_{PSII}, supports the finding that triploid ramets also have greater CO_2 assimilation rates than diploids. Given that iWUE and g_s are greater, it also implies that triploids have much greater A than diploids. This is similar to findings in *Eucalyptus grandis* where increased A (driven by nitrogen fertilization treatments) in the absence of a corresponding change in g_s, resulted in less negative $\delta^{13}C$ and higher iWUE

EPA Author Manuscript

EPA Author Manuscript

EPA Author Manuscript

(Clearwater and Meinzer 2001). However, plants that are more heat and drought tolerant might instead have greater iWUE by decreasing g_s more relative to A, instead of increasing A more relative to g_s. For example, in apple trees, while A measured in 'Fuji' and 'Braeburn' apple tree varietals was similar, g_s was lower and iWUE was greater in the 'Braeburn' variety which is more conservative in its water use (Massonnet et al. 2007). However, relationships between A and g_s are influenced by many factors and plant-scale water use efficiency is not always correlated with leaf-scale iWUE (Seibt et al. 2008).

Conclusion

Given that triploid trees are most frequent across aspen's distribution in warmer and drier climates, and triploids have greater iWUE than diploids, the simplest conclusion is that the greater iWUE in triploid clones provides an advantage in drier climates and possible resilience against mortality. However, because the greater iWUE is attained by both greater A and g_s on a per leaf, as well as a per ramet basis, we suspect that triploid ramets also have greater overall transpiration and therefore would need a greater water supply than diploid ramets. Therefore, at ramet-scale, we expect that drought stress in quaking aspen is mediated by ploidy type, D, and water availability, and that aspen triploids may be more prone to drought or heat stress.

Differences in the relative fitness of each ploidy type relative to climate and water availability are also likely influenced by other factors that we did not study, but we can speculate about diploid-triploid competition in the landscape. For instance, triploids are less conservative with water use at high D, which could provide a carbon uptake advantage to triploids. This could explain why triploid clones (including Pando) typically have higher basal area increments than diploids (DeRose et al. 2014). Furthermore, additional carbon reserves in triploids could potentially allow individual clones to spread over large areas (Mock et al. 2012, Mock et al. 2008). Spreading growth could also allow triploids to maximize the utilization of available water resources, which could be particularly important in the mountainous landscapes of the American West. However, during a severe drought (like the 2002 and 2003 event that caused SAD in the western United States), we reason that triploid aspen ramets might die faster than the more physiologically conservative diploids, though the ploidy type of SAD-affected clones has not been adequately measured to prove or disprove this hypothesis. Future mapping of clone boundaries in stands that experienced SAD, and the identification of the ploidy type of both SAD-affected and healthy co-occurring clones, could provide data to illustrate differences between ploidy levels in growth and water loss. Furthermore, knowing the size and distributions of diploid and triploid clones over larger areas than those that have been studied, along with measurements of ramet density, root-to-shoot ratios and changes to clone boundaries over time, could aid in untangling the evolutionary ecology of the ploidy types in this species. Projections of a warmer and drier climate suggest that SAD events will reoccur in the future (Worrall et al. 2013). Given the structural and functional differences between ploidy types, and that triploid aspen clones are likely sterile and unable to recolonize as easily as wind-dispersed diploid aspens, we might also expect that triploid aspen will be more negatively affected by climate change than diploids.

EPA Author Manuscript

EPA Author Manuscript

EPA Author Manuscript

Forest and land-use management plans, or assisted migration proposals, do not often discuss polyploidy in plants. This may be simply because ploidy measurements are not routine, or because the ecological consequences of intraspecific variation in polyploidy are considered inconsequential compared to interspecific ecological drivers. However, biological, and functional differences between diploid and triploid aspen likely enhance the climate niche of aspen, which occurs across much of North America.

Supplementary Material

Refer to Web version on PubMed Central for supplementary material.

Acknowledgements

We thank Steven Strauss who provided useful insight that guided study methods and interpretations of our data. We are thankful for the support of the Rocky Mountain Biological Laboratory in Gothic, Colorado, who provided funding and logistical support to B. Greer. B. Greer also would like to thank the science director, Jennifer Reithel, and the executive Ian Billick for their support while scoping this project, collecting data, and summarizing our findings. We also thank Jennifer McKay for completing our isotope analysis and we thank Lisa Ganio, Ariel Muldoon, and Jonathon Valente for guidance in our statistical approaches. We thank Steven Voelker who provided useful comments that greatly improved the manuscript. We also thank Brian Dolan, Richard Cronn, and Chris Poklemba who provided access to equipment and guidance for flow cytometry and Patrick Hayes who provided barley leaves. We also thank reviewers for thoughtful and comprehensive reviews that significantly improved the manuscript.

This manuscript has been subjected to Agency review and has been approved for publication. The views expressed in this paper are those of the author(s) and do not necessarily reflect the views or policies of the U.S. Environmental Protection Agency. Mention of trade names or commercial products does not constitute endorsement or recommendation for use.

Funding

Oregon State University and the Rocky Mountain Biological Laboratory.

References

Ally D, Ritland K, Otto SP (2010) Aging in a long-lived clonal tree. PLoS biology. 8

Anderegg LD, Anderegg WR, Abatzoglou J, Hausladen AM, Berry JA (2013a) Drought characteristics' role in widespread aspen forest mortality across Colorado, USA. Glob Chang Biol. 19:1526–37. [PubMed: 23504823]

Anderegg WR, Anderegg LD, Berry JA, Field CB (2014) Loss of whole-tree hydraulic conductance during severe drought and multi-year forest die-off. Oecologia. 175:11–23. [PubMed: 24394863]

Anderegg WR, Berry JA, Smith DD, Sperry JS, Anderegg LD, Field CB (2012) The roles of hydraulic and carbon stress in a widespread climate-induced forest die-off. Proceedings of the National Academy of Sciences of the United States of America. 109:233–7. [PubMed: 22167807]

Anderegg WR, Plavcová L, Anderegg LD, Hacke UG, Berry JA, Field CB (2013b) Drought's legacy: multiyear hydraulic deterioration underlies widespread aspen forest die-off and portends increased future risk. Global Change Biology. 19:1188–1196. [PubMed: 23504895]

Barker MS, Husband BC, Pires JC (2016) Spreading Wings and flying high: The evolutionary importance of polyploidy after a century of study. American journal of botany. 103:1139–45. [PubMed: 27480249]

Bennett M, Leitch I. 2012 Angiosperm DNA C-values database, http://www.kew.org/cvalues/.

Bretfeld M, Franklin SB, Peet RK (2016) A multiple-scale assessment of long-term aspen persistence and elevational range shifts in the Colorado Front Range. Ecological Monographs. 86:244–260.

EPA Author Manuscript EPA Author Manuscript EPA Author Manuscript

Clearwater MJ, Meinzer FC (2001) Relationships between hydraulic architecture and leaf photosynthetic capacity in nitrogen-fertilized Eucalyptus grandis trees. Tree physiology. 21:683–690. [PubMed: 11446997]

Collatz GJ, Ball JT, Grivet C, Berry JA (1991) Physiological and environmental regulation of stomatal conductance, photosynthesis and transpiration: a model that includes a laminar boundary layer. Agricultural and Forest Meteorology. 54:107–136.

Coop JD, Barker KJ, Knight AD, Pecharich JS (2014) Aspen (Populus tremuloides) stand dynamics and understory plant community changes over 46years near Crested Butte, Colorado, USA. Forest Ecol Manag. 318:1–12.

DeRose RJ, Mock KE, Long JN (2014) Cytotype differences in radial increment provide novel insight into aspen reproductive ecology and stand dynamics. Canadian Journal of Forest Research. 45:1–8.

Drake PL, Froend RH, Franks PJ (2013) Smaller, faster stomata: scaling of stomatal size, rate of response, and stomatal conductance. J Exp Bot. 64:495–505. [PubMed: 23264516]

Farquhar GD, O'Leary MH, Berry JA (1982) On the relationship between carbon isotope discrimination and the intercellular carbon dioxide concentration in leaves. Functional Plant Biology. 9:121–137.

Farquhar Gv, Caemmerer Sv, Berry J (1980) A biochemical model of photosynthetic CO2 assimilation in leaves of C3 species. Planta. 149:78–90. [PubMed: 24306196]

Franks PJ, Drake PL, Beerling DJ (2009) Plasticity in maximum stomatal conductance constrained by negative correlation between stomatal size and density: an analysis using Eucalyptus globulus. Plant, cell & environment. 32:1737–1748.

Harley P, Thomas R, Reynolds J, Strain B (1992) Modelling photosynthesis of cotton grown in elevated CO2. Plant, cell & environment. 15:271–282.

Harley PC, Sharkey TD (1991) An improved model of C3 photosynthesis at high CO2: reversed O2 sensitivity explained by lack of glycerate reentry into the chloroplast. Photosynthesis Research. 27:169–178. [PubMed: 24414689]

Hogg EH, Hurdle P (1997) Sap flow in trembling aspen: implications for stomatal responses to vapor pressure deficit. Tree physiology. 17:501–509. [PubMed: 14759823]

Jarvis P (1976) The interpretation of the variations in leaf water potential and stomatal conductance found in canopies in the field. Philosophical Transactions of the Royal Society of London B: Biological Sciences. 273:593–610.

Kemperman JA, Barnes BV (1976) Clone size in American aspens. Canadian Journal of Botany. 54:2603–2607.

Lawson T, Blatt MR (2014) Stomatal size, speed, and responsiveness impact on photosynthesis and water use efficiency. Plant physiology. 164:1556–1570. [PubMed: 24578506]

Li W-L, Berlyn GP, Ashton PMS (1996) Polyploids and their structural and physiological characteristics relative to water deficit in Betula papyrifera (Betulaceae). American journal of botany:15–20.

Ling Q, Huang W, Jarvis P (2011) Use of a SPAD-502 meter to measure leaf chlorophyll concentration in Arabidopsis thaliana. Photosynthesis Research. 107:209–214. [PubMed: 21188527]

Madlung A, Wendel J (2013) Genetic and epigenetic aspects of polyploid evolution in plants. Cytogenetic and genome research. 140:270–285. [PubMed: 23751292]

Maherali H, Walden AE, Husband BC (2009) Genome duplication and the evolution of physiological responses to water stress. New phytologist. 184:721–731. [PubMed: 19703115]

Massonnet C, Costes E, Rambal S, Dreyer E, Regnard JL (2007) Stomatal Regulation of Photosynthesis in Apple Leaves: Evidence for Different Water-use Strategies between Two Cultivars. Annals of botany. 100:1347–1356. [PubMed: 17901058]

Maxwell K, Johnson GN (2000) Chlorophyll fluorescence—a practical guide. Journal of experimental botany. 51:659–668. [PubMed: 10938857]

Mitton JB, Grant MC (1996) Genetic variation and the natural history of quaking aspen. Bioscience. 46:25–31.

Mock KE, Callahan CM, Islam-Faridi MN, Shaw JD, Rai HS, Sanderson SC, Rowe CA, Ryel RJ, Madritch MD, Gardner RS, Wolf PG (2012) Widespread triploidy in Western North American aspen (Populus tremuloides). Plos One. 7:e48406. [PubMed: 23119006]

EPA Author Manuscript EPA Author Manuscript EPA Author Manuscript

Mock KE, Rowe CA, Hooten MB, Dewoody J, Hipkins VD (2008) Clonal dynamics in western North American aspen (Populus tremuloides). Mol Ecol. 17:4827–44. [PubMed: 19140975]

Oren R, Sperry JS, Katul GG, Pataki DE, Ewers BE, Phillips N, Schaefer KVR (1999) Survey and synthesis of intra-and interspecific variation in stomatal sensitivity to vapour pressure defici. Plant Cell and the Environment. 22:1515–1526.

Pärnik T, Ivanova H, Keerberg O, Vardja R, Niinemets Ü (2014) Tree age-dependent changes in photosynthetic and respiratory CO2 exchange in leaves of micropropagated diploid, triploid and hybrid aspen. Tree physiology:tpu043.

Peet RK (1981) Forest vegetation of the Colorado front range. Vegetatio. 45:3–75.

Pinheiro J, Bates D, DebRoy S, Sarkar D, Team RC. 2017 nlme: Linear and Nonlinear Mixed Effects Models Ed. 3.1–131 Rpv.

R Core Team. 2013 R: A Language and Environment for Statistical Computing. R Foundation for Statistical Computing, Vienna, Austria.

Roden JS (2003) Modeling the light interception and carbon gain of individual fluttering aspen (Populus tremuloides Michx) leaves. Trees-Struct Funct. 17:117–126.

Roden JS, Pearcy RW (1993a) The effect of flutter on the temperature of poplar leaves and its implications for carbon gain. Plant, cell & environment. 16:571–577.

Roden JS, Pearcy RW (1993b) Effect of Leaf Flutter on the Light Environment of Poplars. Oecologia. 93:201–207. [PubMed: 28313608]

Roden JS, Pearcy RW (1993c) Photosynthetic Gas-Exchange Response of Poplars to Steady-State and Dynamic Light Environments. Oecologia. 93:208–214. [PubMed: 28313609]

Rogers PC, Gale JA (2017) Restoration of the iconic Pando aspen clone: emerging evidence of recovery. Ecosphere. 8

Schneider CA, Rasband WS, Eliceiri KW (2012) NIH Image to ImageJ: 25 years of image analysis. Nature methods. 9:671–5. [PubMed: 22930834]

Segraves KA, Anneberg TJ (2016) Species interactions and plant polyploidy. American journal of botany. 103:1326–1335. [PubMed: 27370313]

Seibt U, Rajabi A, Griffiths H, Berry JA (2008) Carbon isotopes and water use efficiency: sense and sensitivity. Oecologia. 155:441–454. [PubMed: 18224341]

Sharkey TD (1985) Photosynthesis in intact leaves of C3 plants: physics, physiology and rate limitations. The Botanical Review. 51:53–105.

Soltis DE, Segovia-Salcedo MC, Jordon-Thaden I, Majure L, Miles NM, Mavrodiev EV, Mei WB, Cortez MB, Soltis PS, Gitzendanner MA (2014) Are polyploids really evolutionary dead-ends (again)? A critical reappraisal of Mayrose et al. (2011). New Phytologist. 202:1105–1117. [PubMed: 24754325]

Thornley JH (2002) Instantaneous canopy photosynthesis: analytical expressions for sun and shade leaves based on exponential light decay down the canopy and an acclimated non-rectangular hyperbola for leaf photosynthesis. Annals of botany. 89:451–8. [PubMed: 12096806]

Tyree MT, Patino S, Bennink J, Alexander J (1995) Dynamic Measurements of Root Hydraulic Conductance Using a High-Pressure Flowmeter in the Laboratory and Field. Journal of Experimental Botany. 46:83–94.

White J, Vaughn B (2011) Stable Isotopic Composition of Atmospheric Carbon Dioxide (13C and 18O) from the NOAA ESRL Carbon Cycle Cooperative Global Air Sampling Network, 1990–2012, Version: 2013–04-05. University of Colorado, Institute of Arctic and Alpine Research (INSTAAR) ftp cmdl noaa gov/ccg/co2c13/flask/event/,(last access 21 September 2012)

Worrall JJ, Rehfeldt GE, Hamann A, Hogg EH, Marchetti SB, Michaelian M, Gray LK (2013) Recent declines of Populus tremuloides in North America linked to climate. Forest Ecol Manag. 299:35–51.

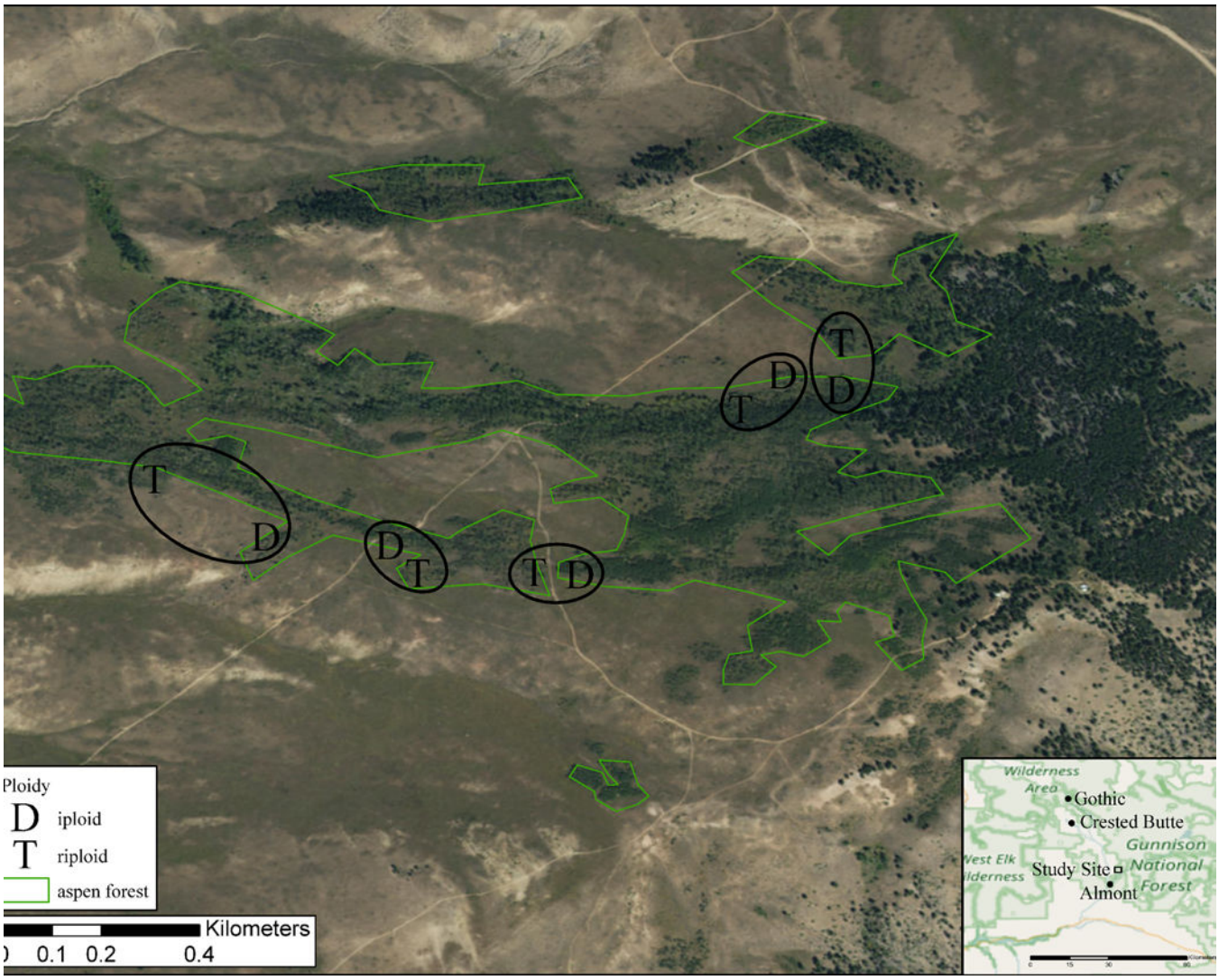

Figure 1.

The study site and the aspen forest surrounding the studied clones. The circles show the locations of paired diploid (D) and triploid (T) clones. Polygons denote the extent of the aspen forest. In the map inset United States National Forest lands and wilderness areas in Colorado are labeled.

EPA Author Manuscript EPA Author Manuscript EPA Author Manuscript

EPA Author Manuscript

EPA Author Manuscript

EPA Author Manuscript

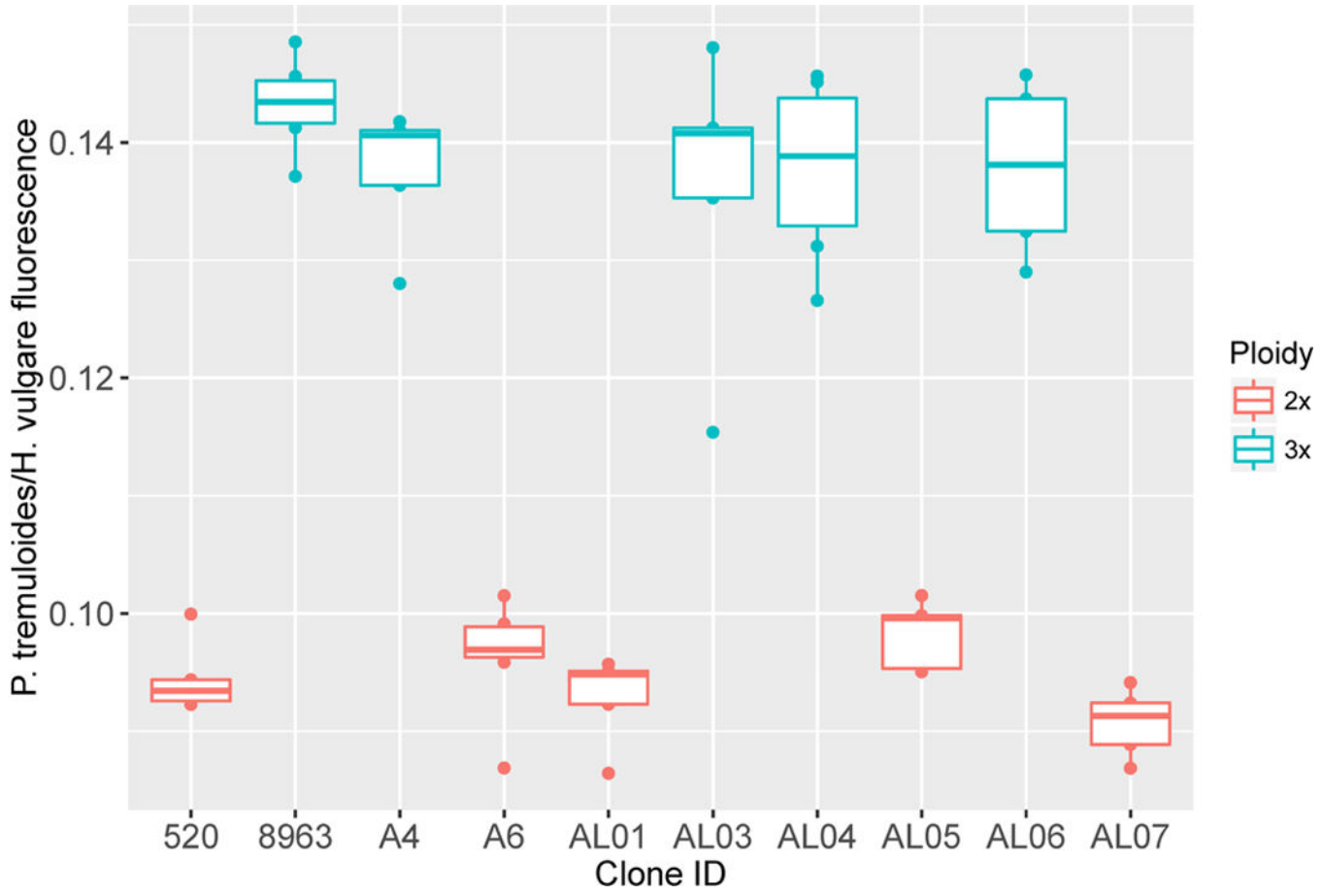

Figure 2.

The ratios of the median peak fluorescence intensity of quaking aspen against barley measured in leaves in each ramet of each clone. Triploid aspen were expected to have a brightness that is 50% greater than that of diploid aspen because, containing one extra copy of their chromosomes, triploid should have 50% more nuclear genetic material than a diploid. 2x is diploid and 3x is triploid.

EPA Author Manuscript

EPA Author Manuscript

EPA Author Manuscript

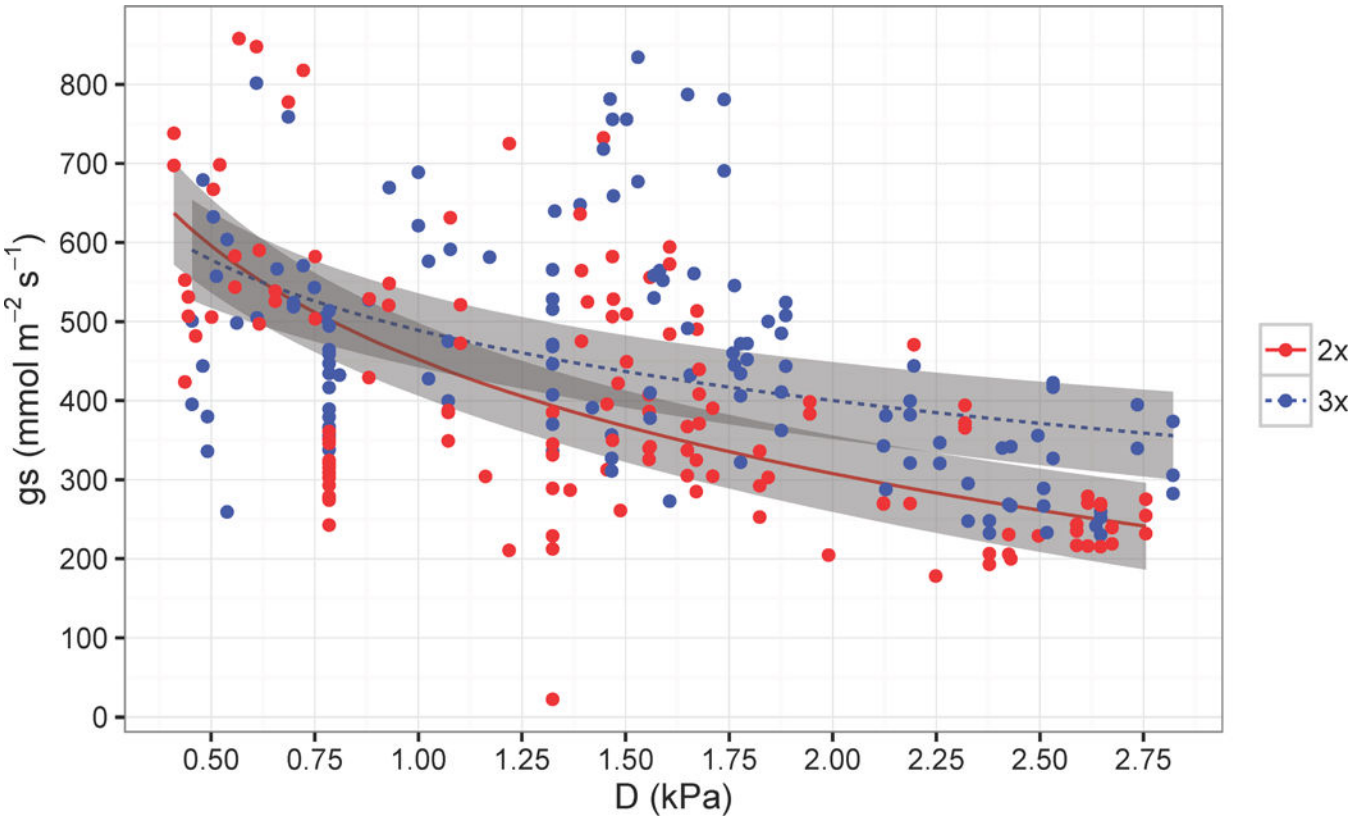

Figure 3.

Stomatal conductance (g_s) as a function of vapor pressure deficit (D). The lines represent the predicted g_s as a function of D from the mixed model and the grey boxes represent standard errors around predictions (2x is diploid and 3x is triploid).

EPA Author Manuscript

EPA Author Manuscript

EPA Author Manuscript

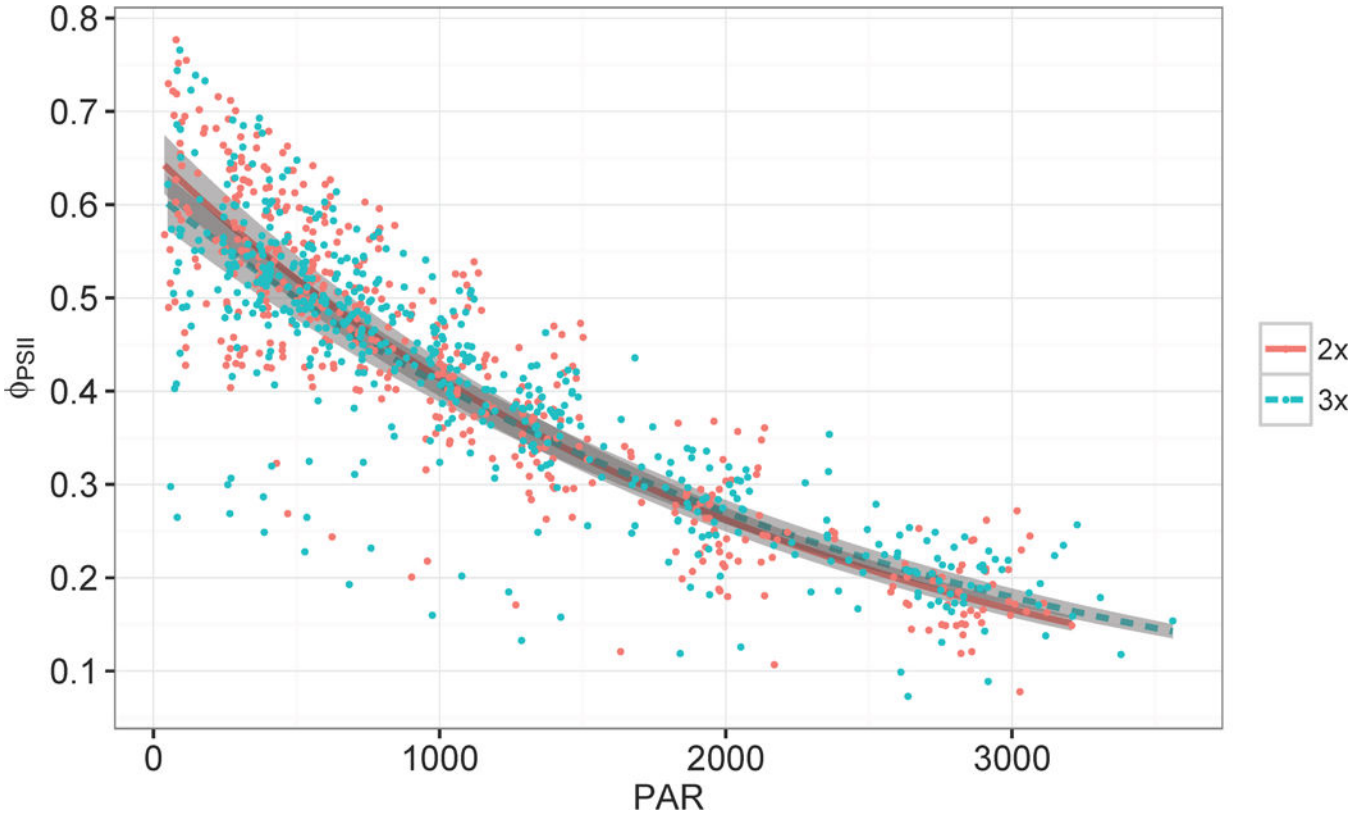

Figure 4.

ΦPSII as a function of PAR for diploid and triploid aspen measured in RLCs. The lines represent diploid and triploid predictions of ΦPSII relative to PAR and the grey boxes represent standard errors around the predictions (2x is diploid and 3x is triploid).

EPA Author Manuscript

EPA Author Manuscript

EPA Author Manuscript

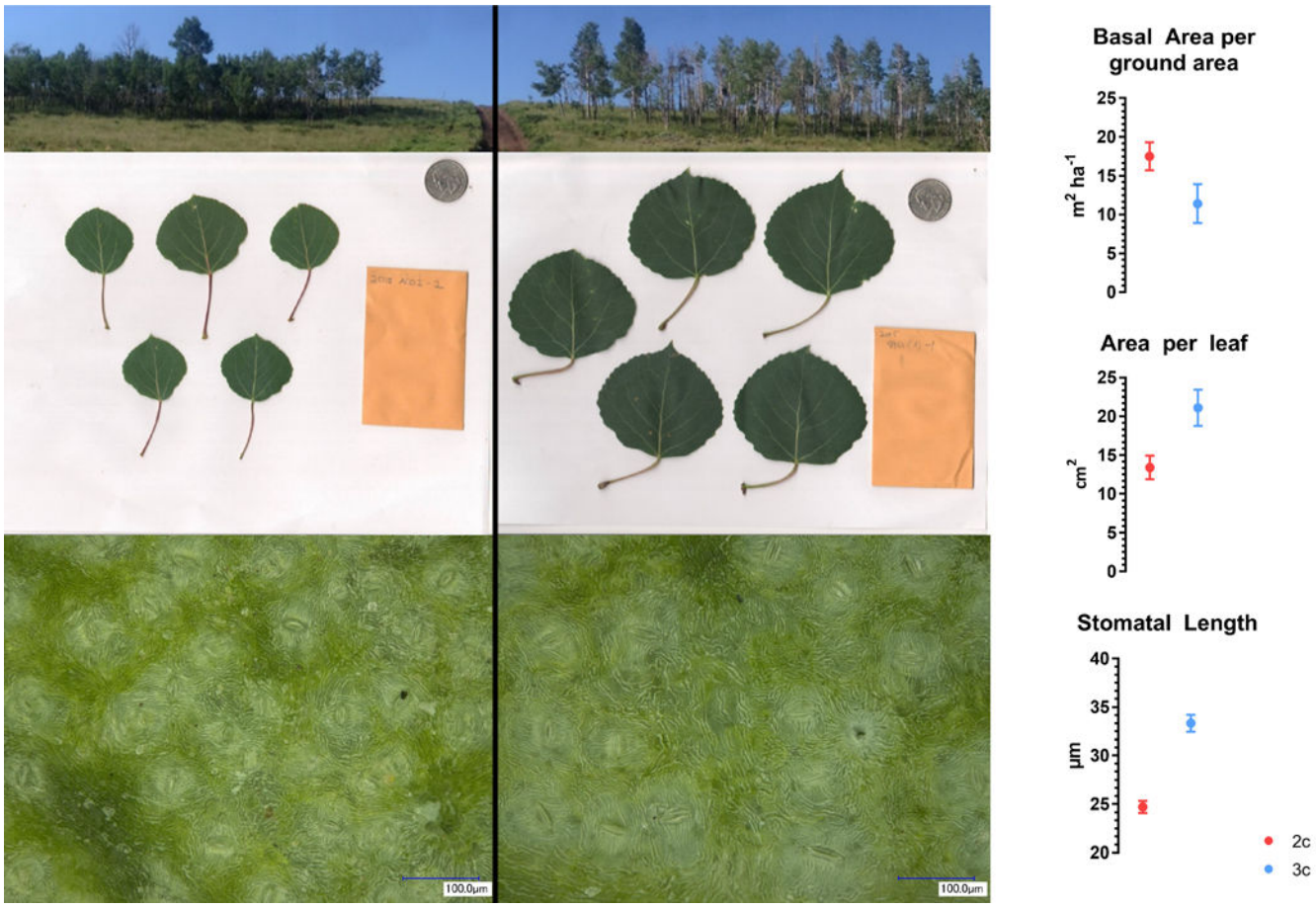

Figure 5.

Images from two adjacent clones in the Almont site show clear differences between diploid (left) and triploid (right) characteristics. Stand density (top), leaf size (middle), and stomatal size (bottom) were all statistically different between ploidy types. Scale bar in bottom row images is 100 μm. Plots depict diploid and triploid means and standard errors (also see Tables 1 and 2).

EPA Author Manuscript EPA Author Manuscript EPA Author Manuscript

Table 1.

Statistics and supporting data from the linear mixed models for the stand and ramet measurements. Standard error included with diploid and triploid mean. Statistically significant values ($p < 0.05$) are in bold.

	Measurement	Diploid	Triploid	Triploid/Diploid Ratio	*F*-statistic	n	*p*-value
Clone Measurements	Basal Area per ground area (m^2 ha^{-1})	**17.5 ± 1.8**	**11.4 ± 2.5**	**0.65**	**$F_{1,8} = 5.86$**	**52**	**0.04**
	Canopy Openness (% open canopy)	28 ± 5	27 ± 8	0.97	$F_{1,8} = 0.01$	52	0.91
Ramet Measurements	DBH (cm)	10.8 ± 1.4	11.0 ± 2.0	1.03	$F_{1,8} = 0.02$	51	0.89
	Ramet Height (meters)	4.7 ± 0.6	5.3 ± 0.9	1.13	$F_{1,8} = 0.53$	51	0.49
	Leaf Area Index (LAI, leaf area per unit ground)	0.8 ± 0.1	0.7 ± 0.1	0.86	$F_{1,8} = 1.08$	42	0.33
	Leaf Area Distal to Branch Segment (cm^2)	432 ± 40	399± 50	0.93	$F_{1,8} = 0.39$	40	0.55
	Hydraulic Conductivity, Kh (kg m^2 s^{-1} MPa^{-1})	$3.6\times10^{-8}\pm 6.0\times10^{-9}$	$4.7\times10^{-8}\pm 8.5\times10^{-9}$	1.31	$F_{1,8} = 1.70$	40	0.23
	Specific Conductivity, Ks (kg m^{-1} s^{-1} MPa^{-1})	$2.1\times10^{-3}\pm 7.4\times10^{-4}$	$3.4\times10^{-3}\pm 1.0\times10^{-3}$	1.60	$F_{1,8} = 1.47$	40	0.26
	Hydraulic Conductivity normalized by leaf area, Kl (kg m^{-1} s^{-1} MPa $^{-1}$)	$1.2\times10^{-6}\pm 3.1\times10^{-7}$	$1.3\times10^{-6}\pm 4.3\times10^{-7}$	1.16	$F_{1,8} = 0.18$	40	0.68

EPA Author Manuscript EPA Author Manuscript EPA Author Manuscript

Table 2.

Statistics and supporting data from the linear mixed models for leaf physiology and function. Statistically significant values ($p < 0.05$) are in bold.

Measurement	Diploid	Triploid	Triploid/Diploid Ratio	n	*F*-statistic	*p* -value
Area per leaf (cm^2)	**13.4 ± 1.5**	**21.1 ± 2.3**	**1.6**	**52**	**$F_{1,8} = 10.82$**	**0.01**
Dry Mass per leaf (grams)	**0.14 ± 0.01**	**0.24 ± 0.02**	**1.76**	**52**	**$F_{1,8} = 24.66$**	**<0.01**
Leaf Mass per Area (LMA, mg cm^{-2})	**10.2 ± 0.3**	**11.5 ± 0.4**	**1.12**	**52**	**$F_{1,8} = 8.17$**	**0.02**
Chlorophyll content (SPAD, a unitless index)	**41.4 ± 2.8**	**53.2 ± 3.9**	**1.28**	**51**	**$F_{1,8} = 8.96$**	**<0.02**
Stomatal length (μm)	**24.7 ± 0.6**	**33.3 ± 0.9**	**1.35**	**52**	**$F_{1,8} = 98.86$**	**<0.01**
Stomatal density (count per mm^2)	58.5± 4.7	53.8 ± 6.6	0.92	52	$F_{1,8} = 0.51$	0.50
Stomatal conductance, g_s, (mmol m^{-2} sec^{-1})	400 ± 19	454 ± 26	1.14	261	$F_{1,8} = 4.29$	0.07
Stomatal conductance, g_s, (mmol m^{-2} sec^{-1}) with log(D) as fixed effect		**Depends on D**		**261**	**$F_{1,193} = 7.35$**	**<0.01**

Tree Physiol. Author manuscript; available in PMC 2019 May 20.

EPA Author Manuscript EPA Author Manuscript EPA Author Manuscript

Table 3.

Statistics from the linear mixed models for measurements and proxies of net assimilation (A). Statistically significant values ($p < 0.05$) are in bold.

	Measurement	Diploid	Triploid	Triploid/Diploid Ratio	n	F-statistic	*p*-value
A/C_i	V_{cmax}	68.7 ± 3.4	69.5 ± 4.9	1.01	22	$F_{1,8} = 0.03$	0.88
	J_{max}	129.0 ± 6.1	145.0 ± 8.6	1.12	22	$F_{1,8} = 3.42$	0.10
	R_d	2.7 ± 0.5	2.1 ± 0.7	0.81	22	$F_{1,8} = 0.47$	0.51
	Γ*	51.2 ± 1.4	48.2 ± 1.9	0.94	22	$F_{1,8} = 2.39$	0.16
	K_m	970.6 ± 43.6	872.9 ± 61.6	0.90	22	$F_{1,8} = 2.52$	0.15
Fluorometry	Φ_{PSII} (Dark adapted)	0.88 ± 0.003	0.89 ± 0.004	1.01	1142	$F_{1,46} = 1.05$	0.31
	Φ_{PSII} (Light adapted)	**Depends on PAR**			**1017**	**$F_{1,902} = 43.57$**	**<0.01**
	J (light adapted)	Depends on PAR			1017	$F_{1,902} = 2.08$	0.15
	July 2015 α (from curves fit individually)	0.31 ± 0.01	0.29 ± 0.01	0.95	110	$F_{1,8} = 1.29$	0.29
	July 2015 ETR_{max} (from curves fit individually)	302.2 ± 18.2	319.4 ± 25.7	1.06	110	$F_{1,8} = 0.45$	0.52
	June 2016, α (from curves fit individually)	0.31 ± 0.02	0.34 ± 0.02	1.10	18	$F_{1,2} = 1.82$	0.31
	June 2016, ETR_{max} (from curves fit individually)	113.9 ± 8.4	161.0 ± 11.8	1.41	18	$F_{1,2} = 15.98$	<0.06

EPA Author Manuscript EPA Author Manuscript EPA Author Manuscript

Table 4.

Statistics from the linear mixed models for measurements and calculated values related to iWUE and A. Statistically significant values ($p < 0.05$) are in bold.

Measurement	Diploid	Triploid	Triploid/Diploid Ratio	n	F-statistic	*p*-value
$\delta^{13}C$	**−27.5 ± 0.2**	**−26.5 ± 0.3**	**0.97**	**63**	**$F_{1,8} = 12.87$**	**<0.01**
C_i	**258.4 ± 3.3**	**241.6 ± 4.7**	**0.94**	**63**	**$F_{1,8} = 12.87$**	**<0.01**
C_i/C_a	**0.65 ± 0.01**	**0.61 ± 0.01**	**0.94**	**63**	**$F_{1,8} = 12.87$**	**<0.01**
iWUE	**86.9 ± 2.1**	**97.4 ± 2.9**	**1.12**	**63**	**$F_{1,8} = 12.87$**	**<0.01**
Leaf N % mass	2.2 ± 0.1	2.4 ± 0.1	1.08	63	$F_{1,8} = 4.99$	<0.06
Leaf C% mass	47.7 ± 0.5	46.9 0.7	0.98	63	$F_{1,8} = 1.17$	0.31
C:N	21.4 ± 0.6	19.5 ± 0.8	0.91	63	$F_{1,8} = 4.99$	<0.06
Average mass of leaf nitrogen per leaf area (mmol m^{-2})	**163 ± 6**	**196 ± 8**	**1.20**	**10**	**$F_{1,8} = 15.34$**	**<0.01**
Total average mass of nitrogen per leaf (mmol)	**0.2 ± 0.04**	**0.4 ± 0.05**	**1.91**	**10**	**$F_{1,8} = 13.63$**	**<0.01**